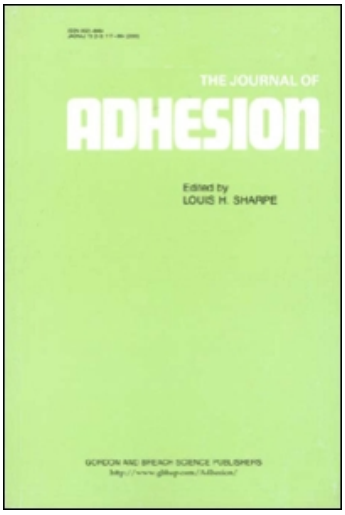

The Journal of Adhesion
Publication details, including instructions for authors and subscription information:
http://www.informaworld.com/smpp/title~content=t713453635

Analysis of Interaction between RuO_2 and Glass by Growth of RuO_2 Particles in Glasses

T. Nakano[a]; K. Suzuki[a]; T. Yamaguchi[a]
[a] Faculty of Science and Technology, Keio University, Yokohama, Japan

To cite this Article Nakano, T. , Suzuki, K. and Yamaguchi, T.(1994) 'Analysis of Interaction between RuO_2 and Glass by Growth of RuO_2 Particles in Glasses', The Journal of Adhesion, 46: 1, 131 — 144
To link to this Article: DOI: 10.1080/00218469408026655
URL: http://dx.doi.org/10.1080/00218469408026655

J. Adhesion, 1994, Vol. 46, pp. 131–144
Reprints available directly from the publisher
Photocopying permitted by license only

Printed in the United States of America

Analysis of Interaction between RuO_2 and Glass by Growth of RuO_2 Particles in Glasses*

T. NAKANO, K. SUZUKI and T. YAMAGUCHI

Faculty of Science and Technology, Keio University, 3-14-1, Hiyoshi, Kohoku-ku, Yokohama, 223, Japan

(Received October 20, 1992; in final form April 13, 1993)

The RuO_2-glass interaction has been studied by analyzing the growth of RuO_2 particles in glasses. The size of RuO_2 particles was determined by TEM and X-ray line broadening. The RuO_2/glass interfacial energy was evaluated by spreading and penetration experiments.

Changes in size and shape of RuO_2 particles indicated that coarsening proceeded by the diffusion-controlled dissolution-precipitation process. The growth rate of RuO_2 particles at temperatures giving the same viscosity was dependent on the glass composition. Kinetics of the Ostwald ripening and values of glass surface energy implied that the solubility of RuO_2 in glass is a critical factor. Results indicated that the solubility of RuO_2 in glass decreases with increasing PbO content and with increasing SiO_2 substitution for B_2O_3. Dissolution of Al_2O_3 from substrate retarded the Ostwald ripening.

KEY WORDS RuO_2; glass; thick film; wetting; solubility; particle coarsening; electronics; resistors.

INTRODUCTION

RuO_2-glass composites have been used in electronic applications such as thick film resistors. The resistivity varies over several orders of magnitude with RuO_2 content. The relation between RuO_2 content and resistivity depends on the glass composition and firing temperature, and can not be explained completely by percolation theory.[1–4] Chemical interaction between RuO_2 and glass is a possible factor responsible for the resistivity variation. Therefore, information on the interaction is useful to control better the electrical properties of RuO_2-glass thick film resistors.

The RuO_2-glass interaction was studied by analyzing the growth of RuO_2 particles in glasses of various compositions. The RuO_2/glass interfacial energy was estimated from spreading and penetration experiments. The growth behavior of RuO_2 particles provides valuable information on dissolution and the diffusion of RuO_2 in glass as well as on the RuO_2/glass interfacial energy. Ostwald ripening of RuO_2 particles

*Presented at the International Symposium on "The Interphase" at the Sixteenth Annual Meeting of The Adhesion Society, Inc., Williamsburg, Virginia, U.S.A., February 21–26, 1993.

in glass was reported by Prabhu[5] and Prudenziati,[6] but sufficient information is not available for studying the chemical interaction.

EXPERIMENTAL

1. Materials

Pastes containing various volume fractions of RuO_2 particles were prepared by mixing RuO_2 particles, glass powder, and organic binder with a Fuber Muller mixer. Six compositions of glasses were used. The compositions and densities of the glasses are shown in Table I. Figure 1 illustrates the temperature-viscosity curves of glasses

TABLE I
Compositions and densities of glasses

	Composition (mol%)						Density
	SiO_2	Al_2O_3	B_2O_3	PbO	BaO	CaO	(g/cm^3)
A1	48.6	4.9	13.8	32.7	0	0	4.6
A2	53.2	5.3	15.2	26.3	0	0	3.7
A3	58.8	5.9	16.8	18.5	0	0	3.4
B1	50.2	2.7	7.9	0	0	39.2	2.3
C1	20.0	2.0	50.0	0	20.0	0	4.0
C2	20.0	2.0	50.0	20.0	0	0	3.0

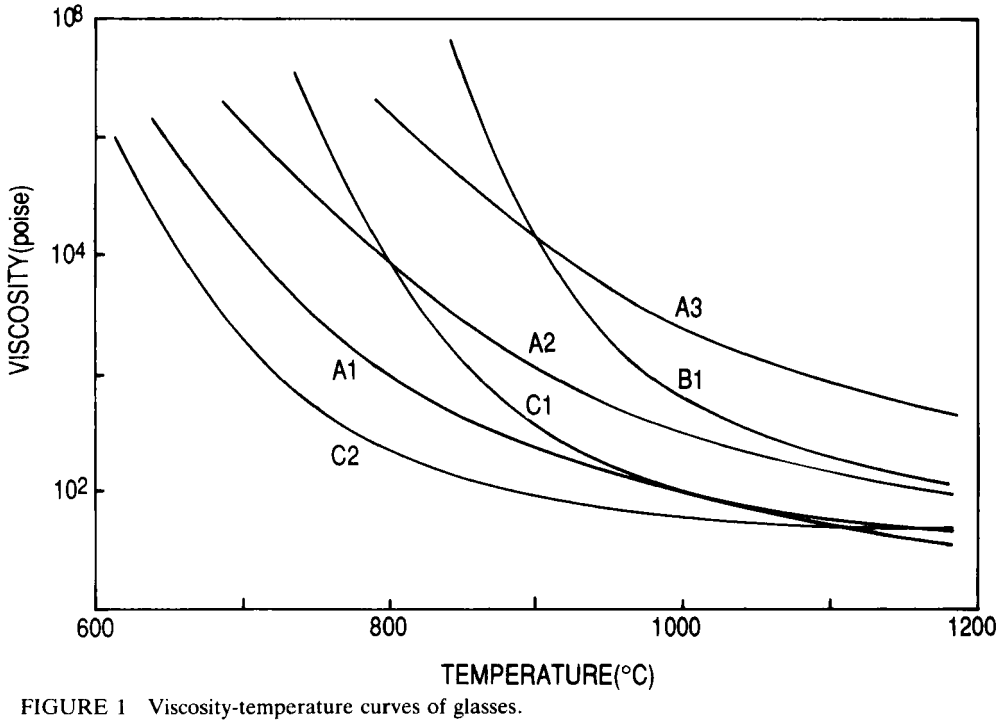

FIGURE 1 Viscosity-temperature curves of glasses.

determined with a rotating-cup type viscometer. The particle size distribution and shape of RuO_2 particles are shown in Figures 2a and 3a, respectively. The organic vehicle was prepared from 90wt% diethyleneglycol-mono-n-butylether and 10wt% ethyl cellulose. Pastes were printed on 20 μm thick Pt foils and 96wt% Al_2O_3 substrates, dried and heated. The RuO_2-glass films were 10 μm thick after heating.

2. Particle Size of RuO_2

The average particle size of RuO_2 was determined by TEM and X-ray line broadening. For TEM observations Ar^+ beam-thinning was applied to the bottom of the Pt foil. The particle sizes were calculated from areas of RuO_2 particles in TEM images. The particle size was measured also by X-ray line broadening of the (110) plane using the Scherer equation.

3. RuO_2/Glass Interfacial Energy

The RuO_2/glass interfacial energy was estimated from kinetics of spreading and penetration. Variation in the diameter of glass beads on RuO_2 thin films was observed as a function of time during isothermal heating. The RuO_2 thin films were prepared by sputtering Ru on Al_2O_3 substrates and subsequent oxidation. The weight of a glass bead was 20.5 mg. Glass beads were made from fragments of glass pellets by heating and subsequent grinding. The glass melt penetrated into the film of RuO_2 particles. The distance of isothermal penetration was measured as a function of time. A 20 μm thick RuO_2 film was formed on a 20 μm thick glass film formed by printing on the Al_2O_3 substrate and heating at 800°C for 10 min.

RESULTS AND DISCUSSION

1. Ostwald Ripening of RuO_2 Particles in Glass

As shown in Figure 2, the obtained size distributions were compared with the theoretical ones[7,8] derived from both diffusion- and reaction-controlled mechanisms. The diffusion-controlled mechanism better accounted for the actually-obtained distributions than the reaction-controlled mechanism. However, the obtained distribution did not completely agree with the basic theoretical distribution[7,8] or any modified theoretical distributions.[10–16] This fact suggests that the coarsening process in this system is more complex than that theoretically assumed. Extensive growth is observed at 950°C.

Figure 3 also indicates that RuO_2 particles grew by the dissolution-precipitation mechanism. As shown in Figure 3, RuO_2 particles rounded as temperature increased, indicating that RuO_2 particles dissolved in the glass. The absence of neck growth in the contact areas between RuO_2 particles denies the possibility of material transport through interparticle contact areas.

Figure 4 illustrates the isothermal growth kinetics. The linear relation between r^3 and t implies that the growth is diffusion-controlled. The basic theory of the Ostwald

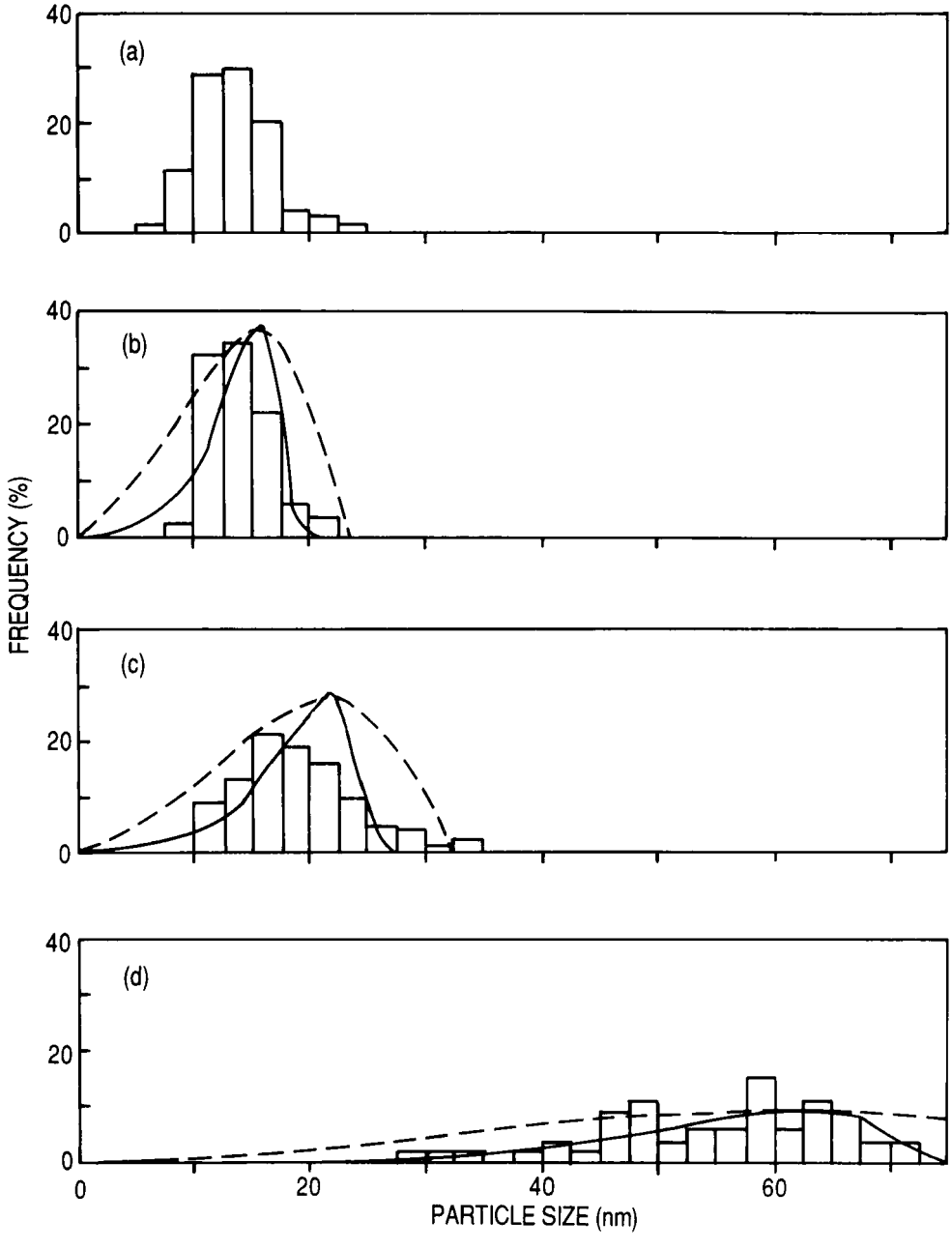

FIGURE 2 Effect of temperature on the size distribution of RuO_2 particles. 10 vol% RuO_2, determined by TEM, (a) starting RuO_2 particles, and heated in glass C2 on Pt foil for 1 hr at: (b) 700°C; (c) 850°C; (d) 950°C, solid lines and dotted lines indicate theoretical distribution of diffusion- and reaction-controlled particle coarsening mechanism, respectively, calculated from obtained average particle size.

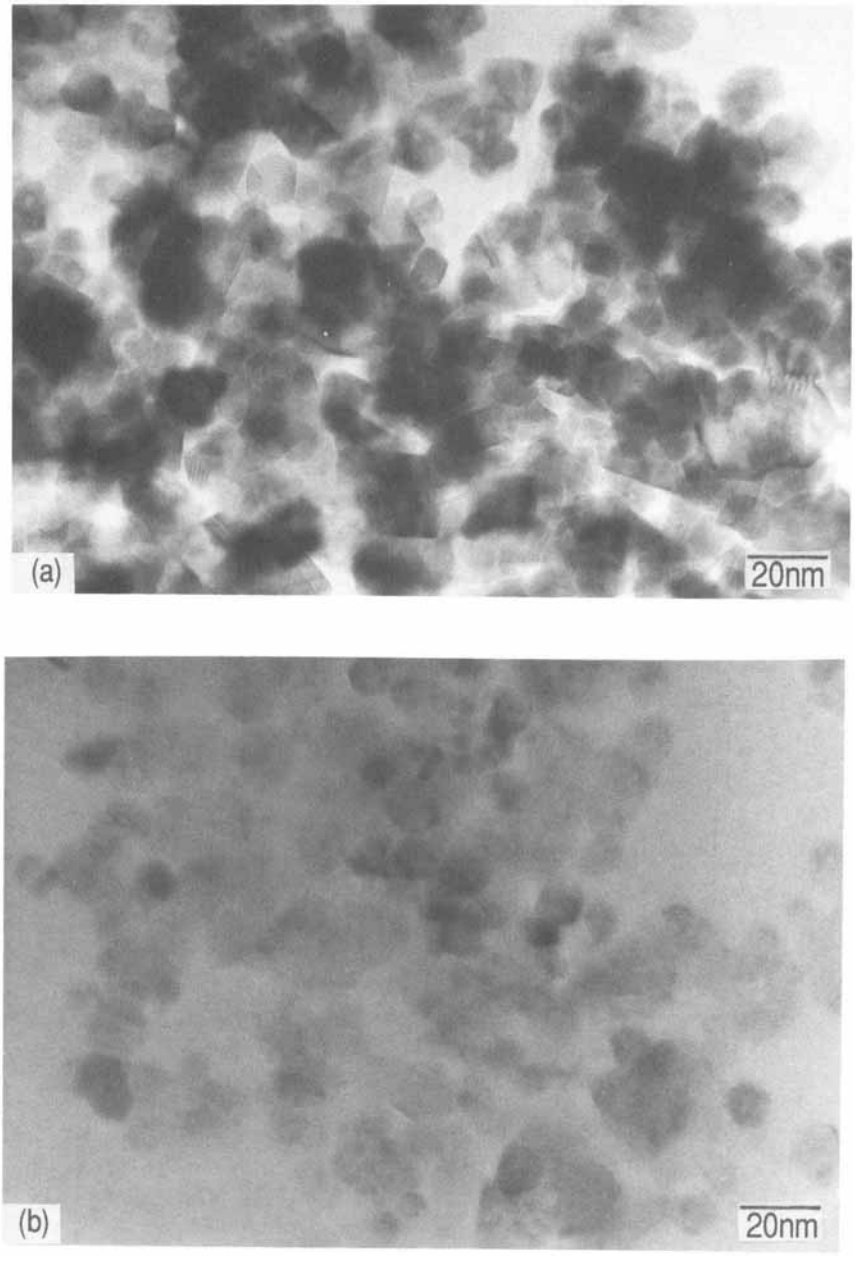

FIGURE 3 Effect of temperature on the growth of RuO_2 particles. 10 vol% RuO_2, observed by TEM, (a) starting RuO_2 particles, and heated in glass C2 on Pt foil for 1 hr at: (b) 700°C; (c) 850°C; (d) 950°C.

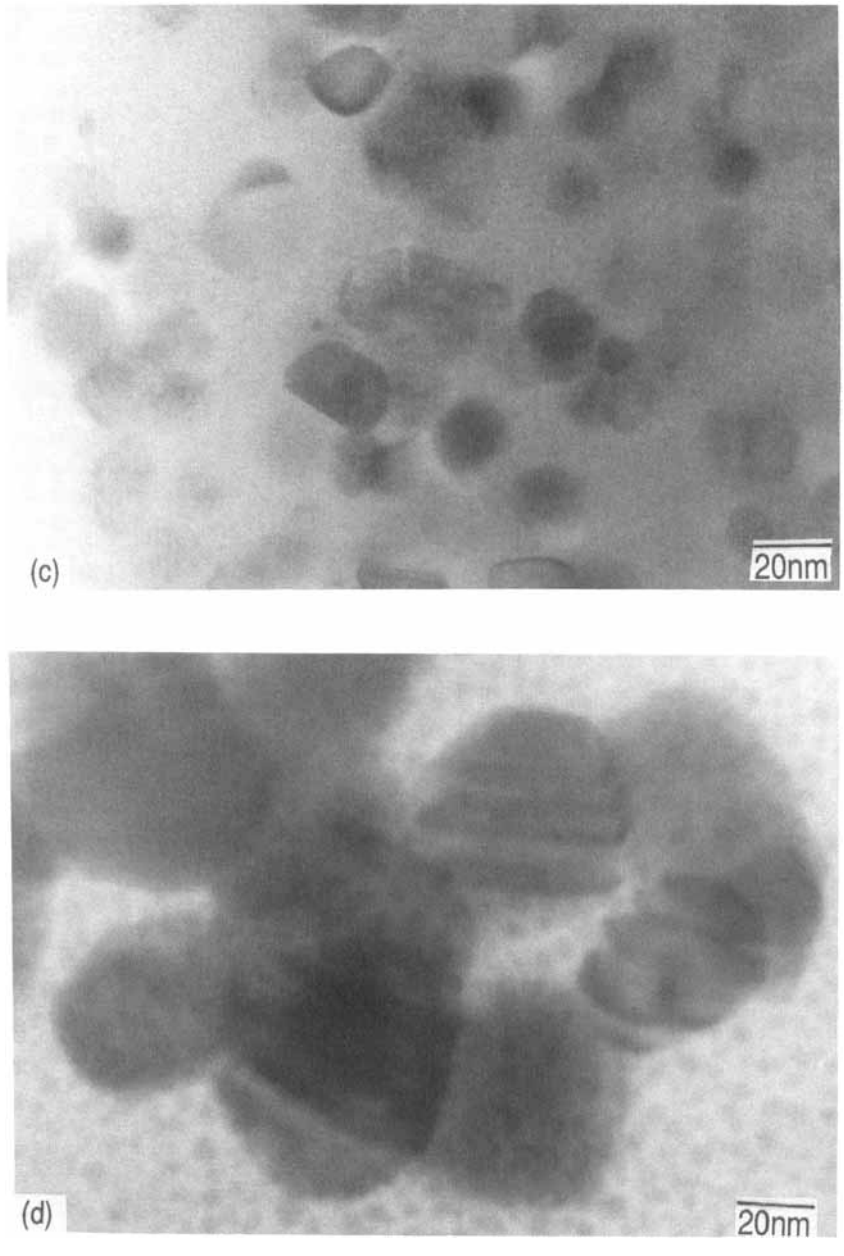

FIGURE 3 *(Continued)*

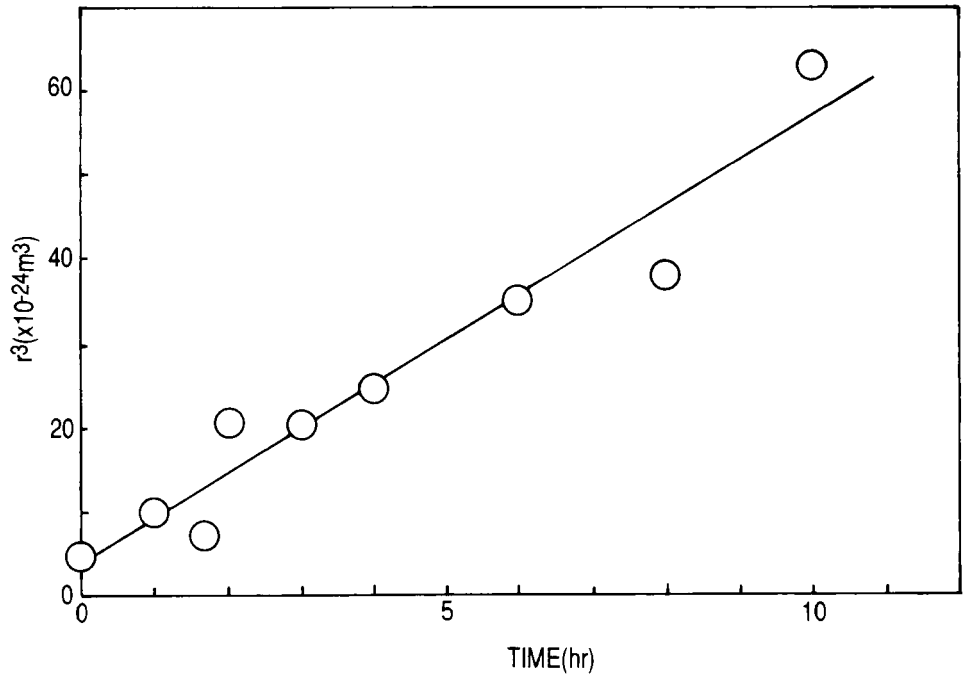

FIGURE 4 Effect of heating time on the growth of RuO_2 particles. 10 vol% RuO_2, determined by X-ray line broadening, heated in glass A2 on Pt foil for 1 hr at 950°C.

ripening will be briefly discussed. The theory of diffusion-controlled Ostwald ripening claims[7-10] that the average particle radius, r, increases with time, t, according to equation (1),

$$r^3 - r_0^3 = C_G t \tag{1}$$

where r_0 is the average radius at the onset of the Ostwald ripening and C_G is the growth rate constant given by:

$$C_G = \frac{8\gamma_{SL} CDV^2}{9RT} \tag{2}$$

where γ_{SL} is the particle/matrix interfacial energy, C is the solute concentration in equilibrium with a particle of infinite radius, D is the diffusion coefficient, V is the molar volume of precipitate, R is the gas constant, and T is the heating temperature.

Equations (1) and (2) assume that the volume fraction of the precipitate is essentially zero. Several modifications[10-16] were proposed to predict the relation between rate constant and volume fraction.

2. Effect of Glass Composition on the Ostwald Ripening

The contributions of the viscosity, η, solubility, C, and interfacial energy, γ_{SL}, to C_G will be discussed, so that the effect of glass composition may be understood. C_G

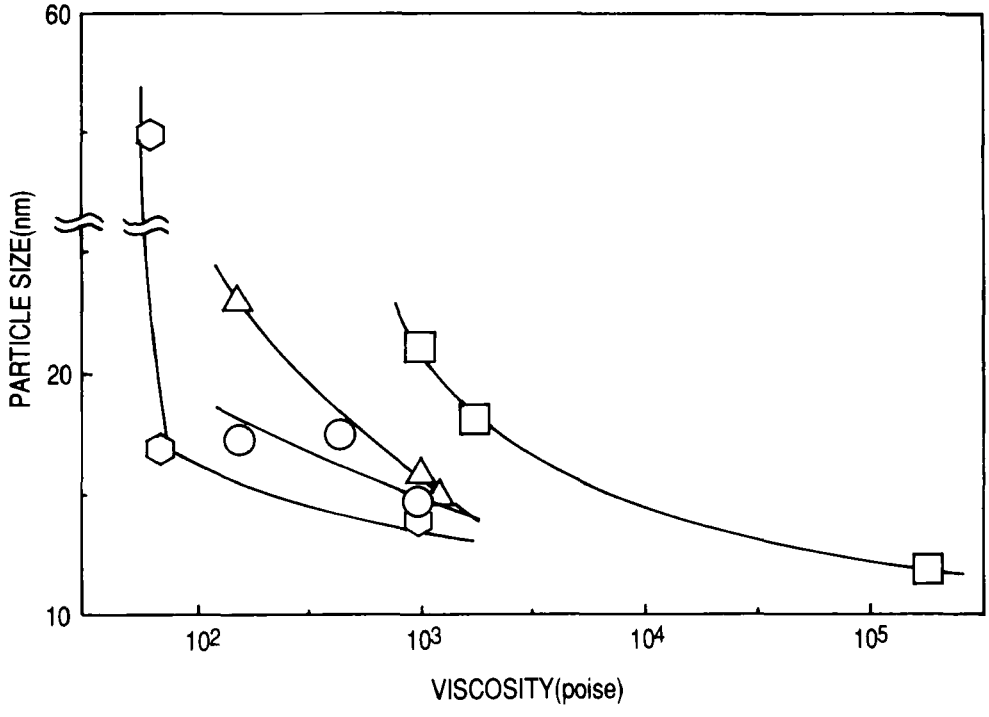

FIGURE 5 Effect of glass viscosity on the growth of RuO_2 particles. 10 vol% RuO_2, determined by TEM, heated on Pt foil for 1 hr in glasses: ○A1; □B1; △C1; ○C2.

is a function of viscosity, η, solubility, C, and interfacial energy, γ_{SL}, as expressed by,

$$C_G = \frac{4\gamma_{SL}CV^2}{27\pi\eta} \tag{3}$$

because the diffusion constant D is given by Stokes-Einstein equation:

$$D = \frac{RT}{6\pi\eta}. \tag{4}$$

Figure 5 illustrates the effect of glass viscosity on the particle size of RuO_2 for different glass compositions. The data in Figure 5 indicate that the viscosity is not the only factor governing the growth behavior. Growth rate constants at temperatures corresponding to the viscosity of 10^3 poise are shown in Table II. The rate constant

TABLE II
Rate constants of the Ostwald ripening

	A1	A2	A3	B1	C1	C2
k	20	75	70	194	49	8

($\times 10^{-29} m^3/s$), from Fig. 5, $\eta = 10^3$ poise.

is the largest for glass B1 and the smallest for glass C2. The particle size increases with decreasing viscosity but its dependence on the viscosity is different. It is to be noted that the particle size at the viscosity of 10^3 poise (glass B1) is smaller than that of the original particles. Probably only dissolution is operative under this condition.

The RuO_2/glass interfacial energy, γ_{SL}, was estimated by the spreading and penetration experiments. The diameter of a spreading glass bead was measured at temperatures giving the same viscosity of 10^3 poise. Acording to Dodge[17] the diameter of a liquid droplet, d, at time, t, is given as,

$$d^7 - d_i^7 = C_S t \tag{5}$$

where d_i is the initial diameter of the droplet and C_S is the rate constant of spreading given by:

$$C_S = K\frac{\gamma_{LV} V_0^2}{\eta} \tag{6}$$

where V_0 is the volume of the droplet, K is a nondimensional parameter and γ_{LV} is the surface tension of glass. Figure 6 shows the relation between t and d^7. The rate constant of spreading, C_S, was determined from the plots by assuming that d^7 increases linearly with time. The surface tension, γ_{LV}, was calculated from the rate constant of spreading, C_S. The constant K was assumed to be 1.5 because K varied over a range from 0.5 to 2.5 for the complete set of 112 tests and the bulk of

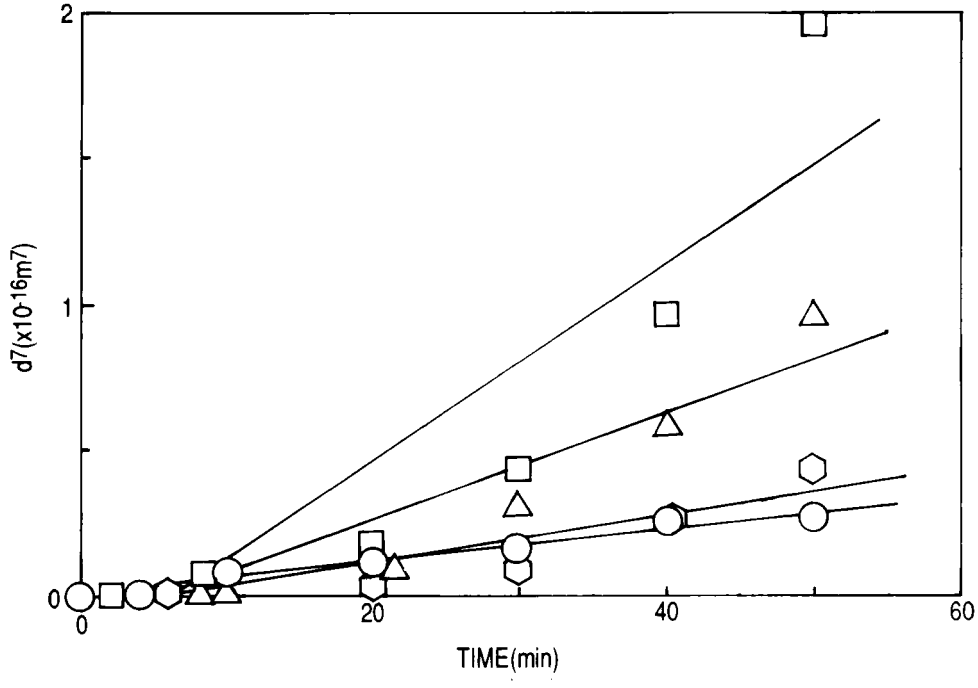

FIGURE 6 Effect of glass composition on the spreading kinetics. Heated on RuO_2 thin films at temperatures giving a viscosity of 10^3 poise, glasses: ○A1; □B1; △C1; ○ C2.

TABLE III
Surface tensions of glasses

	A1	A2	B1	C1	C2
γ_{LV}	0.3	0.1	0.6	0.6	0.4

(J/m^2), from Fig. 6, $\eta = 10^3$ poise.

tests clustered around $K = 1.5$.[17] The surface tension calculated from the spreading kinetics shown in Table III is twice as large as those of lead borosilicate and barium borosilicate glasses.[18] However, it is possible to compare the values from the spreading experiment qualitatively. The surface tensions for lead-free glasses (B1 and C1) are larger than those for lead-containing ones (A1, A2 and C2) in Table III. The penetration distance was measured at temperatures giving viscosities of 10^3 and 10^4 poise. Equation (7) describes the penetration distance, l, as a function of time, t,[19-20]

$$l^2 = C_p t \tag{7}$$

where C_p is the rate constant of penetration given by:

$$C_p = \frac{a^2}{4\eta}\left(\frac{2\gamma_{LV}\cos\theta}{a} + \Delta P\right) \tag{8}$$

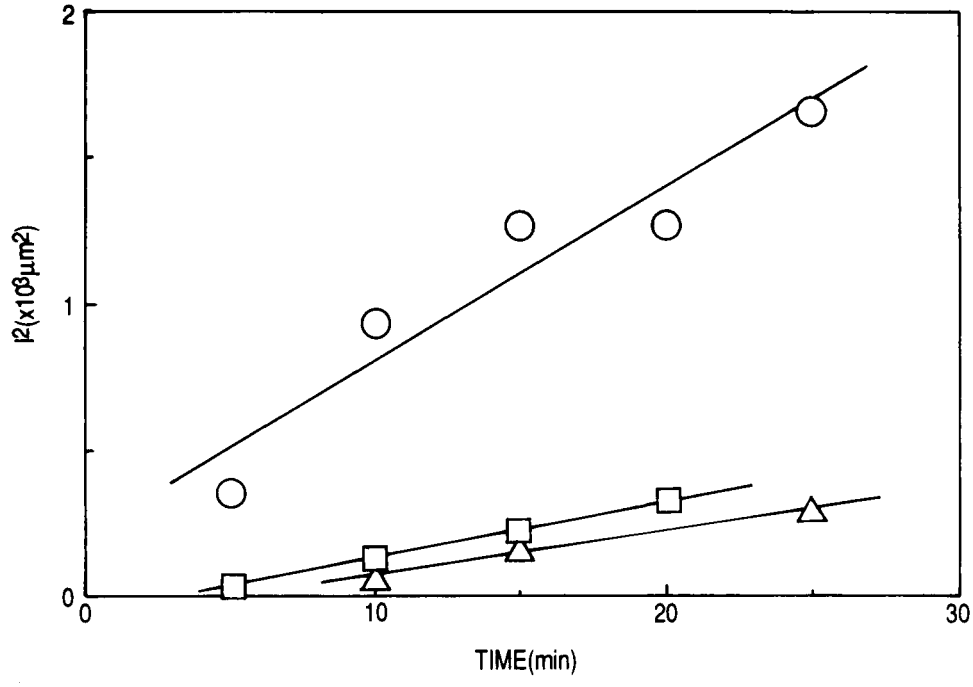

FIGURE 7 Effect of glass composition on the penetration kinetics. Heated at temperatures giving a viscosity of 10^3 poise, glasses: ○A1; □C1; △C2.

TABLE IV
Rate constants of penetration

η(poise)	A1	C1	C2
10^3	320	255	947
10^4	7	3	25

($\times 10^{-15} m^2/s$), from Fig. 7.

where a is the average pore radius of the RuO_2 film, ΔP is the total pressure difference between top and bottom of the RuO_2 film, and the contact angle, θ, is 0. Values of l^2 for glasses A1, C1, and C2 were linearly related with t as shown in Figure 7. Table IV shows the rate constants of penetration determined by experiments. Equation (8) indicates that γ_{LV} increases with increasing C_p. Table IV also indicates that the surface tension for lead-free glass C1 is larger than that for lead-containing glasses A1 and C2. The RuO_2/glass interfacial energy can be estimated from Young's equation.

$$\gamma_{SL} = \gamma_{SV} - \gamma_{LV} \cos \theta. \tag{9}$$

γ_{SL} decreases with increasing γ_{LV} because γ_{SV} is almost constant in the temperature range studied.

The solubility of RuO_2 in glass will be discussed with the growth rate constant and RuO_2/glass interfacial energy. A decrease in γ_{SL} implies the retarded growth of RuO_2 particles, because the growth rate constant, C_G, is proportional to γ_{SL} (eq. 2). The observed results were in contradiction to the prediction; glass B1 gave the largest growth rate constant in spite of the small RuO_2/glass interfacial energy. The above discussion suggests that the solubility is a critical factor responsible for the growth. Thus, we presume that the growth rate constant depends on the solubility of RuO_2 in glass. On the basis of this view, the effect of glass composition on the solubility was studied. Comparison of rate constants between glasses C1 and C2 indicates that the solubility decreases with increasing PbO substitution for BaO. Furthermore, increase in PbO content (glasses A2 and A1) and increasing B_2O_3 substitution for SiO_2 (glasses A3 and C2) will decrease the solubility.

It is suggested from the rate constant that the solubility of RuO_2 increases with increasing basicity of glass. The solubilities and basicities for glasses B1 and C1 are larger than those for glasses A1 and C2. Vest[4] reported the same tendency; that is, that the solubility of RuO_2 in a potassium borate glass is larger than that in a lead borosilicate glass.

We tried to measure the solubility of RuO_2 in glasses by the ICP-AES solution method, but we were not able to determine it because of the extremely low solubility (less than 500 ppm).

3. Effect of Substrate on the Ostwald Ripening

The effect of the substrate material on the growth of RuO_2 particles is illustrated in Figure 8. The size of RuO_2 particles heated in glass C2 on an Al_2O_3 substrate was compared with that heated on a Pt foil. At 700° and 850°C, the sizes of RuO_2

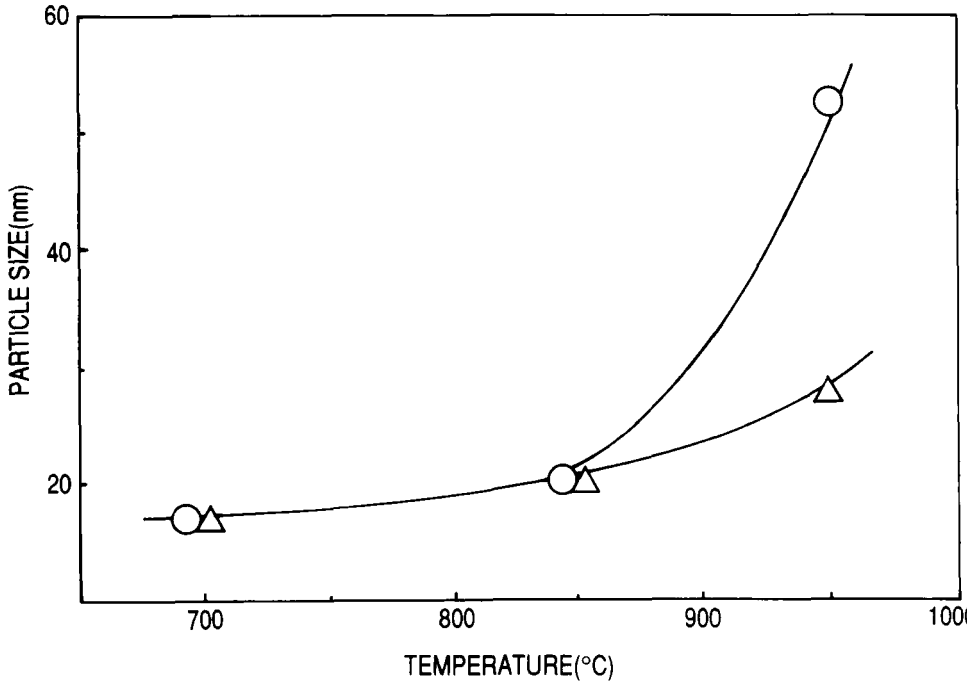

FIGURE 8 Effect of substrate material on the growth of RuO_2 particles. 10 vol% RuO_2, determined with X-ray line broadening, heated for 1 hr in glass C2 on: ○Pt foil; △Al_2O_3 substrate.

particles on both substrates were almost the same. At 950°C, however, the size for the Al_2O_3 substrate was much smaller than that for the Pt foil. The Al_2O_3 substrate retarded the growth of RuO_2 particles in glass A2 at 950°C also.

From Figure 8, it is suggested that the growth of RuO_2 particles was retarded as Al_2O_3 dissolved in glass C2. The growth rate constant increases with decreasing viscosity of glass. The viscosity of glass should increase with increasing Al_2O_3 content. Thus, dissolution of Al_2O_3 was studied by EPMA and is shown in Figure 9. The dissolution starts at 700°C and the glass becomes saturated with Al_2O_3 at 950°C for 1 hr. The retarded growth of RuO_2 particles on the Al_2O_3 substrate can be explained by the dissolution of Al_2O_3, resulting in an increase in viscosity. No information is available on the effect of Al^{3+} ion on the solubility of RuO_2 in glass. However, this effect should be insignificant, since Al_2O_3 is an amphoteric compound.

SUMMARY

Coarsening of RuO_2 particles in glass proceeded by the diffusion-controlled dissolution-precipitation mechanism. The results of Ostwald ripening and spreading experiments indicate that the solubility of RuO_2 in glass is a critical factor in the Ostwald ripening of RuO_2 particles. It is suggested that the solubility increases

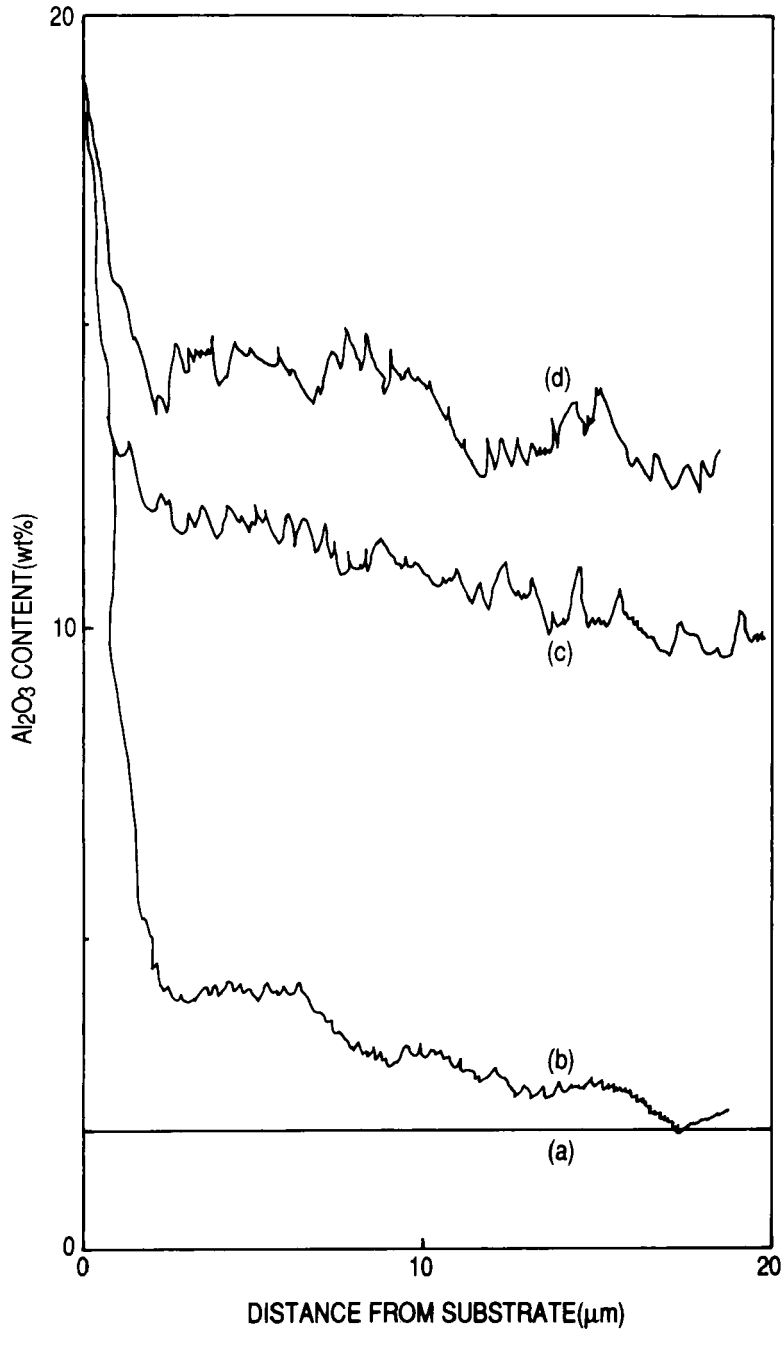

FIGURE 9 Dissolution of Al_2O_3 into glass C2. Measured by EPMA, (a) before heating, and heated for 1 hr at: (b) 700°C; (c) 850°C; (d) 950°C.

with increasing PbO substitution for BaO, increasing PbO content and increasing SiO_2 substitution for B_2O_3. Dissolution of Al_2O_3 in glass retarded Ostwald ripening.

Acknowledgment

The authors express their thanks to Sumitomo Metal Mining Co. Ltd., for EPMA measurement and financial support.

References

1. D. S. McLachlan, M. Blaszkiewicz and R. E. Newnham, *J. Am. Ceram. Soc.* **73,** 2187 (1990).
2. P. J. S. Ewen and J. M. Robertson, *J. Phys. D: Appl. Phys.* **14,** 2253 (1981).
3. P. F. Carcia, A. Ferretti and A. Suna, *J. Appl. Phys.* **53,** 5282 (1982).
4. R. W. Vest and B. S. Lee, IMC 1990 Proc. Tokyo, 83 (1990).
5. A. N. Prabhu and R. W. Vest, *Mater. Sci. Res.* **10,** 399 (1975).
6. M. Prudenziati, B. Morten, F. Cilloni, G. Ruffi and M. Succhi, *J. Appl. Phys.* **65,** 146 (1989).
7. C. Wagner, *Z. Elektrochem.* **65,** 581 (1961).
8. I. M. Lifshitz and V. V. Slyozov, *Phys. Chem. Solids* **11,** 35 (1961).
9. G. W. Greenwood, *Acta Metall.* **4,** 243 (1956).
10. C. S. Jayanth and P. Nash, *J. Mater. Sci.* **24,** 3041 (1989).
11. A. J. Ardell and R. B. Nicholson, *J. Phys. Chem. Solids* **27,** 1793 (1966).
12. D. J. Chellman and A. J. Ardell, *Acta Metall.* **22,** 577 (1974).
13. A. D. Brailsford and P. Wynblatt, *Acta Metall.* **27,** 489 (1979).
14. P. W. Voorhees and M. E. Glicksman, *Metallurgical Trans. A.* **15A,** 1081 (1984).
15. M. Tokuyama and K. Kawasaki, *Physica* **123A,** 386 (1984).
16. J. A. Marqusee and J. Ross, *J. Chem. Phys.* **80,** 536 (1984).
17. F. T. Dodge, *J. Colloid Interface Sci.* **121,** 154 (1987).
18. N. P. Bansal and R. H. Doremus, *Handbook of Glass Properties* (Academic Press Inc., Orlando, 1986), p. 121.
19. B. H. Kaye and M. R. Jackson, *Powder Technol.* **1,** 33 (1967).
20. S. Newman, *J. Colloid Interface Sci.* **26,** 209 (1968).